Shojaei et al. 2013. *Int. J. Vehicle Structures & Systems*, 5(3-4), 109-120
ISSN: 0975-3060 (Print), 0975-3540 (Online)
doi: 10.4273/ijvss.5.3-4.06

International Journal of Vehicle Structures & Systems
Available online at www.maftree.org/eja

Theoretical and Experimental Investigation of Magneto-Rheological Damper based Semi-Active Suspension Systems

Alisina Shojaei[a], H. Metered[b], Siamak Shojaei[c] and S. Olutunde Oyadiji[d]

[a]*WMG Centre for High Value Manufacturing Catapult,*
Warwick University, Coventry, UK.
Email: s.shojaei@warwick.ac.uk

[b]*Faculty of Engineering – Mataria, Helwan University, Cairo, Egypt.*
Corresponding Author, Email: hassan.metered@yahoo.com

[c]*Department of Electrical and Computer Engineering,*
Ohio State University, Columbus, USA.
Email: shojaei.4@osu.edu

[d]*School of Mechanical, Aerospace and Civil Engineering,*
Manchester University, Manchester, UK.
Email: s.o.oyadiji@manchester.ac.uk

ABSTRACT:

Semi-active vehicle suspension systems with Magneto-Rheological (MR) dampers have recently received an increasing attention. Satisfactory performance of these systems is highly dependent on the adopted control method. This paper offers theoretical and experimental investigation of the control of vehicle suspension systems using a quarter car suspension equipped with a MR damper. To achieve the best performance, a control method made of two nested controllers is used. Fuzzy logic, skyhook and On-Off control techniques are studied as system controllers in conjunction with a Heaviside step function as the damper controller. For the theoretical study, the modified Bouc-Wen model of MR dampers is used to calculate the damping force and a mathematical model of the semi-active quarter car suspension is derived and used in the simulation. To prove the applicability of the proposed fuzzy logic controller in a real suspension system, a two degrees of freedom quarter car test rig is designed and used. To quantify the effectiveness of the system under bump and random road disturbance, various performance criteria are evaluated based on the dynamic response of the quarter car suspension system in time and frequency domains,. Simulation and experimental results from the system with the fuzzy logic controllers are compared to the results from the system with skyhook controller, On-Off controller, a passive MR damper and a conventional passive damper.

KEYWORDS:

Semi-Active suspension; Magneto-Rheological damper; Fuzzy logic controller; Ride comfort; Vehicle stability

CITATION:

A. Shojaei, H. Metered, S. Shojaei and S.O. Oyadiji. 2013. Theoretical and Experimental Investigation of Magneto-Rheological Damper based Semi-Active Suspension Systems, *Int. J. Vehicle Structures & Systems*, 5(3-4), 109-120. doi:10.4273/ijvss.5.3-4.06.

1. Introduction

Suspension systems are proved to be the main contributor to the ride comfort and vehicle handling [1]. Apart from the suspension mechanism, typical vehicle suspension system is made up of a spring and a shock absorber or damper. While the spring is chosen solely based on vehicle weight, the shock absorber specifies suspension's position on the ride-handling curve. For a better ride, a soft shock absorber is required to isolate the passengers from unwanted vibrations and dissipate the shock energy transmitted from the road. A harder setting is necessary to ensure better vehicle handling capabilities [2]. The trade-off between these opposing characteristics is a major concern to automotive engineers. Generally, the damping of suspension system is selected according to the particular applications of the vehicle. The conventional suspension systems are therefore passive units which retain a constant setting throughout their lifetime. Hence, they have irresistible performance deficiencies. A solution to this limitation is using active or semi-active suspension (SAS) systems in which a controller forces the suspension to follow the behaviour of some reference system. In an active suspension system, the damper is replaced by a force actuator that minimizes roll and pitch of the automotive body in various driving situations. The cost and complexity of electromechanical actuators and other components used in fully active suspensions are the obstacles standing in the way of their commercial adoption. The viable alternatives are the SAS systems which produce controllable damping and are nearly as efficient as an active suspension and at the same time economically preferable. They are also safer since SAS systems can continue to work as a passive unit in case of a control system failure [3, 4].

In the early SAS dampers, the damping was adjusted by controlling the flow rate of the damping fluid through electrically driven valves. In modern SAS dampers, magneto-rheological (MR) damping fluids are used which when subjected to magnetic fields, can reversibly and instantaneously change from a free-flowing liquid to a semi-solid with controllable yield strength and therefore produce variable damping forces to the suspension [5]. SAS systems with MR dampers have received considerable attention due to the properties of MR dampers such as mechanical simplicity, high dynamic range, low power requirements, large force capacity and robustness [6], and have been shown to be the ultimate solution for achieving the vehicle ride comfort and stability requirements [7, 8].

MR damper is a SAS control device, since only the voltage is applied to the damper's electromagnet that can be controlled directly. The performance of SAS systems is highly dependent on the adopted control strategy. The following two nested controllers are required to control suspension systems with MR damper:

(i) A system controller that specifies the desired damping force for the required performance of the suspension system;

(ii) A damper controller that determines the required damper voltage such that the actual damping force tracks the desired force.

Numerous studies have focused on developing enhanced system controllers for SAS systems and the following different control strategies have been proposed:

- Skyhook controller [8-13];
- H_∞ controller [14];
- Adaptive nonlinear controller [15];
- Neural networks [16];
- Linear quadratic Gaussian control [17, 18];
- Sliding mode control [19, 20];
- Fuzzy logic algorithms [21-24].

The most basic MR damper controller algorithm is the Heaviside step function (HSF) method, in which the applied voltage is either zero or a maximum value. This method was first introduced by Dyke et al. [25] to research the application of MR damper in controlling the structural vibrations due to seismic loads. Biglarbegian et al. [26] verified the effectiveness of a Heaviside step function damper controller together with an adaptive neuro-fuzzy inference system controller in structural control problem.

In this paper, a method identical to Biglarbegian et al. [26] is adopted. The rest of this paper is organized into the following sections. Section 2 describes the dynamics and parameters of a 2 Degrees of freedom (DoF) quarter car model used as the reference system in this study. In Section 3, details of the control methods are discussed. Section 4 is devoted to the numerical model of the MR damper used in simulations. The simulation results are presented and discussed in Section 5. Section 6 explains the details of the experimental setup and results followed by some conclusions.

2. Quarter car model overview

Fig. 1 illustrates a 2 DoF quarter car system model that consists of vehicle body mass, m_b, as sprung mass and vehicle wheel mass, m_w, as unsprung mass. Using Newton's second law, the dynamics of this system can be described by,

$$k_s(y_w - y_b) + f = m_b \ddot{y}_b \tag{1a}$$

$$k_t(y_r - y_w) + k_s(y_b - y_w) - f = m_w \ddot{y}_w \tag{1b}$$

Where y_b and y_w represent the displacement of the body mass and wheel mass respectively. k_s is the suspension stiffness. k_t is the tyre stiffness when the tyre damping is neglected. f is the damping force which can be from conventional passive or SAS damper and is given by,

$$f = \begin{cases} C_s(\dot{y}_w - \dot{y}_b) & \text{for passive suspension} \\ f_a & \text{for SAS} \end{cases} \tag{2}$$

Where C_s is the suspension damping coefficient. The parameters of the model [27] are given in Table 1.

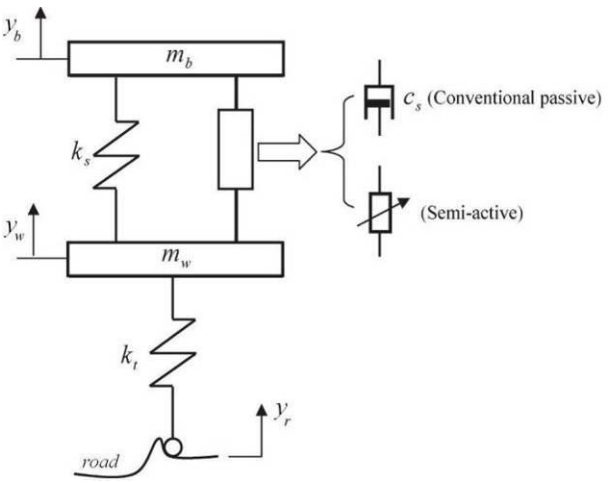

Fig. 1: 2 DoF quarter car model

Table 1: Quarter car model parameters [27]

Parameter	Symbol	Value
Sprung mass	m_b	240 kg
Unsprung mass	m_w	36 kg
Suspension stiffness	K_s	16 kN/m
Damping coefficient	C_s	980 Ns/m
Tyre stiffness	K_t	160 kN/m

3. Control of SAS system

Fig. 2 shows the complete SAS system model which consists of suspension model, system controller, damper controller and MR damper model. In this model, the dynamic response of the quarter car model is passed to the system controller that seeks to enhance the system performance by calculating the desired damping force based on the input data. However, the system controller does not account for the MR damper properties and limitations. Thus the controller output, f_{ctrl}, is an ideal damping force rather than the actual damping force delivered to the system. At the next stage, the damper controller compares the actual damper force, f_a, with f_{ctrl} and adjusts the voltage applied to the MR damper to produce a damping force that tracks f_{ctrl}. The voltage v given to the damper along with the presumed damper displacement ($y = y_b - y_w$) taken from the quarter car suspension, determines the system damping force. Often y is referred to as suspension working space (SWS).

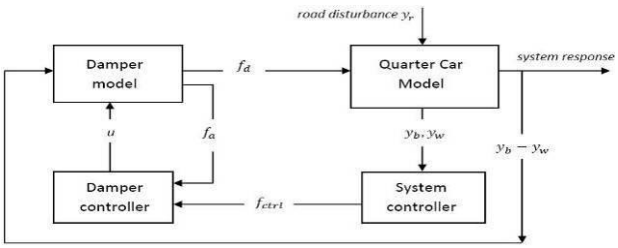

Fig. 2: Components of SAS numerical model

3.1. Skyhook system controller

The skyhook control scheme was patented in 1974 by Karnopp [28]. This controller adjusts the sprung mass and seeks to maximize passenger comfort. The equivalency for this algorithm is a hypothetical damper that connects the sprung mass to a fixed frame in the sky as shown in Fig. 3. The skyhook controller regulates the damper force such that $f_d = C_{sky}\, \upsilon_b$. Where υ_b is the body velocity and C_{sky} is the damper gain in Ns/m. However in reality, a fixed point in the sky is not available on the vehicle. As a result, the effect of ideal skyhook controller on the sprung mass is produced by using a controllable damper connected between the sprung and unsprung masses. The skyhook control algorithms can be mathematically described by:

$$f_{sky} = \begin{cases} C_{sky}\upsilon_b & \text{for } \upsilon_b\upsilon_r > 0 \\ 0 & \text{for } \upsilon_b\upsilon_r \le 0 \end{cases} \tag{3}$$

Where υ_r is the relative velocity of sprung and unsprung masses. When the body moves upwards and the damper is in extension, i.e. υ_b>0, υ_r>0, and the controller activates the damper to push the body mass downwards. When the body moves upwards and the damper is in compression, i.e. υ_b>0, υ_r<0 (υ_w>0 and $|\upsilon_w|>|\upsilon_b|$), the desired damping direction is not consistent with the possible damper force direction since the direction of damper force is determined by the damper relative velocity; υ_r. Hence, the switching law in Eqn. (3) turns the damper off to minimize its negative effect.

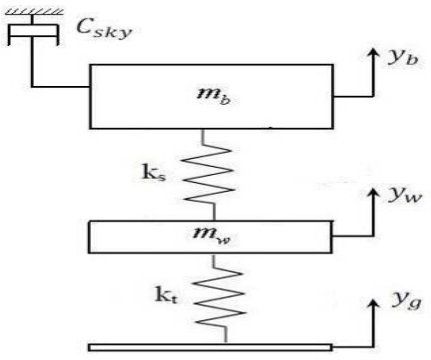

Fig. 3: Skyhook configuration

3.2. On-Off system controller

The damping force in a system with passive damper tends to increase the body mass acceleration when it is in the same direction with spring force. Thus, the damper should ideally produce a minimal force in this condition. The On-Off system control is numerically expressed as:

$$C = \begin{cases} C_{\max} & \text{for } y_r\upsilon_r < 0 \\ C_{\min} & \text{for } y_r\upsilon_r > 0 \end{cases} \tag{4}$$

Where y_r is the relative displacement. C_{max} and C_{min} are the maximum and minimum damping coefficients respectively.

3.3. Fuzzy logic system controller

The fuzzy logic controller takes the relative velocity and relative acceleration of the sprung and unsprung masses as the input variables and specifies the desired damping coefficient of the MR damper. The controller membership functions are shown in Fig. 4. The fuzzy logic variables are categorized as Positive Big (PB), Positive (P), Medium (M), Negative (N) and Negative Big (NB) for input variables and Very Big (VB), Big (B), Medium (M), Small (S) and Very Small (VS) for the output variable. The fuzzy logic rules are defined according to Table 2.

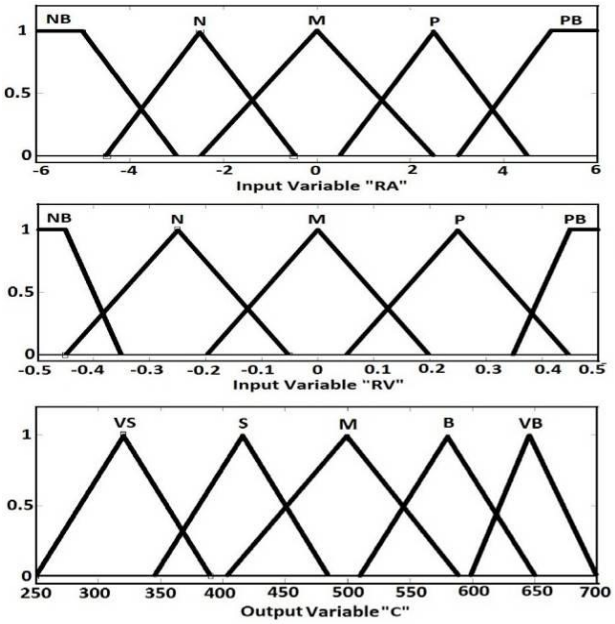

Fig. 4: Fuzzy logic membership functions

Table 2: Fuzzy logic rule base

Output variable C		Input variable RV				
		NB	N	M	P	PB
Input variable RA	NB	VB	B	M	S	VS
	N	B	B	M	S	S
	M	M	M	M	M	M
	P	S	S	M	B	B
	PB	VS	S	M	B	VB

The fuzzy logic controller is based on Mamdani inference method which uses the minimum operation for fuzzy implication and a minimum-maximum operator in composition. The damping membership degree after inference given by,

$$\mu_{C'}(C) = \underset{i=1}{\overset{n}{\vee}} \mu_{C'}(C) = \underset{i=1}{\overset{n}{\vee}} \left[\alpha_i \wedge \mu_{C_i}(C)\right] \tag{5}$$

$$\alpha_i = \mu_{A_i}(a) \wedge \mu_{\upsilon_i}(\upsilon) \tag{6}$$

Where a, υ and C are the crisp values of relative acceleration, relative velocity and damping ratio and μ_{A_i}, μ_{υ_i} and μ_{C_i} are their corresponding membership degrees in the i^{th} rule respectively. $\wedge$ and $\vee$ denote Min and Max operators respectively. Selecting the centroid

defuzzification method and assuming a crisp set $S = \{C | \mu_{C'}(C) > 0\}$, the real-time damping coefficient is given by,

$$\tilde{C} = \frac{\int C\mu_{C'}(C)dC}{\int \mu_{C'}(C)dC} \quad (7)$$

Once the desired damping coefficient is specified, the desired damping force can be defined as a function of the relative velocity.

3.4. Damper controller

The MR damper can be only controlled by regulating the input voltage. For the purpose of this research, a Heaviside step function damper controller is used in which the applied voltage takes either of the two possible values, the minimum value 0 or the maximum value V_{max} and is determined according to the following algorithm:

$$v = V_{max} H\{(f_{ctrl} - f_d) f_d\} \quad (8)$$

Where $H(.)$ is the Heaviside function governed by,

$$H(z) = \begin{cases} 1 & \text{for } z \geq 0 \\ 0 & \text{for } z < 0 \end{cases} \quad (9a)$$

$$\lim_{z \to 0^+} H(z) = 1 \quad (9b)$$

$$\lim_{z \to 0^-} H(z) = 0 \quad (9c)$$

Thus, if the actual damping force generated by the damper is equal to the controller force, the voltage applied to the damper is kept at its current value. When the actual force is less than the controller force in magnitude but in the same direction, the voltage is set to maximum to increase the damping. Otherwise, the applied voltage is zero. Based on previous investigations [6, 20], the maximum applied voltage of the damper controller is set to 2 V.

4. Damper model

The modified Bouc-Wen model for MR dampers is used for simulation purposes in this research. For the system shown in Fig. 5, the damper force is estimated by the following equations [5],

$$f_a = c_1\dot{x} + k_1(y - y_0) \quad (10)$$

$$\dot{x} = \frac{1}{c_0 + c_1}\left[\alpha z + c_0\dot{y} + k_0(y - x)\right] \quad (11)$$

$$\alpha = \alpha(u) = \alpha_a + \alpha_b u \quad (12a)$$

$$c_1 = c_1(u) = c_{1a} + c_{1b} u \quad (12b)$$

$$c_0 = c_0(u) = c_{0a} + c_{0b} u \quad (12c)$$

$$\dot{z} = -\gamma|\dot{y} - \dot{x}||z|^{n-1} z - \beta(\dot{y} - \dot{x})|z|^n + \delta(\dot{y} - \dot{x}) \quad (13)$$

$$\dot{u} = -\eta(u - v) \quad (14)$$

Where x is the internal displacement of the MR damper. u is the output of a first order filter. v is the voltage applied to the current driver. z is an evolution variable to account for the hysteretic effects. k_1 represents the accumulator stiffness. k_0 is the stiffness at high velocity. c_0 and c_1 indicate the amount of viscous damping in high and low velocities respectively. x_0 includes the effect of accumulator. The scale and shape of the hysteresis loop is adjusted by γ, β, δ and η. All the damper model parameters are given in Table 3. In order to solve Eqn. (10) for f_a, Eqns. (11) to (14) must be solved simultaneously with Eqn. (1). Thus three more variables (x, z, u) are introduced.

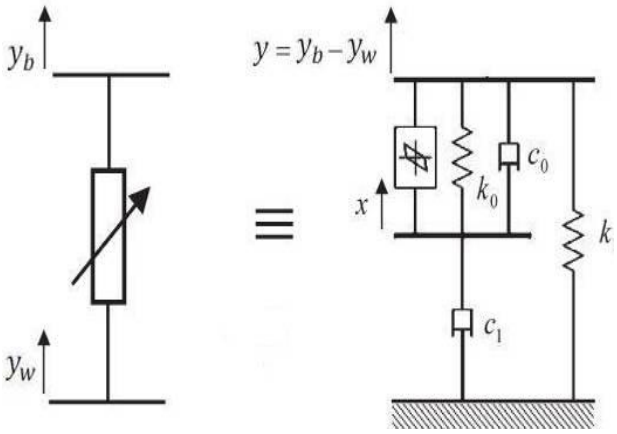

Fig. 5: Modified Bouc-Wen Model adapted for quarter car suspension system model

Table 3: Bouc-Wen parameters [5]

Symbol	Value	Symbol	Value
c_{0a}	784 (Ns/m)	α_a	12441 (N/m)
c_{0b}	1803 (Ns/Vm)	α_b	38430 (N/Vm)
k_0	3610 (N/m)	γ	136320 (m^{-2})
c_{1a}	14649 (Ns /m)	β	2059020 (m^{-2})
c_{1b}	34622 (Ns/Vm)	δ	58
k_1	840 (N/m)	n	2
x_0	0.0245 (m)	η	190 s^{-1}

5. Simulation results and discussions

In vehicle suspension system design, performance criteria vary based on the vehicle type and applications. In the case of passenger cars, the main criteria [20] used to assess the ride quality and stability of the vehicle are SWS, vertical body acceleration (BA) and dynamic tyre load (DTL). The SWS is limited by the structural characteristics of the vehicle. However within the permissible range, if SWS is large, the passengers are more affected by the road roughness. Vehicle ride is greatly affected by the accelerations of vehicle body. In fact, human body is more sensitive to acceleration rather than velocity. Vehicle handling is dependent on the dynamic deformations in the tyre. It is more practical to measure DTL=$K_w(y_g - y_w)$ rather than the dynamic deformations. Vehicle designers thus seek to minimize SWS, BA and DTL simultaneously. The performances of suspension system simulations for the following five cases are detailed:

(i) Conventional passive damping;
(ii) SAS system with skyhook controller;
(iii) SAS system with On-Off controller;
(iv) SAS system with fuzzy logic controller;
(v) MR passive off, i.e. the damper current driver is turned off.

Two types of road excitations are carefully selected to resemble ordinary road profiles [29]. The first excitation, normally used to reveal the transient response characteristics, is a road bump described as:

$$y_g = \begin{cases} a\{1-\cos[\omega_\gamma(t-0.5)]\} & \text{for} \quad 0 \le t \le 0.5+\dfrac{d}{V} \\ 0 \quad \text{Otherwise} \end{cases} \quad (15)$$

Where a is the half-bump amplitude. d is the bump width. V is the vehicle velocity and $\omega_\gamma = \pi V/d$. These parameters are set to: a = 0.035 m, d = 0.8 m, and V = 0.856 m/s. The road excitation signal is shown in Fig. 6(a). Time histories of SWS, BA and DTL responses under this road excitation are plotted in Fig. 6(b)-(c) and Fig. 7(a)-(c) for the five scenarios described earlier. All control types have been able to improve the performance compared to a passive MR damper. This is especially more noticeable in terms of the SWS. These results clearly show that the proposed fuzzy logic controlled suspension can dissipate the energy due to the bump excitation very well. It reduces the settling time and improves both the ride comfort and vehicle stability. The peak to peak (PTP) values of the system response are summarized in Table 4 which shows that SAS systems have led to lower peaks in the SWS, BA and DTL demonstrating their effectiveness at improving ride and stability of the vehicle. When comparing the SWS, BA and DTL criteria, the fuzzy logic controller shows a better performance compared to the other controllers and significantly improved the suspension response. It is also worth noting that the passive MR damper performance is better than the conventional damper.

As explained by Metered et al. [20], the choice of speed (0.856 m/s) is a challenging scenario for the suspension system, particularly with regards to the ride comfort. By repeating the calculations for twice and four times the above speed, it is verified that the fuzzy logic controller still gives a superior performance. For example, when the vehicle runs at twice the chosen speed (i.e. 1.73 m/s), the SWS value recorded for the fuzzy logic controller is 0.054 m which is noticeably smaller than the value recorded for the skyhook controller, 0.061 m and On-Off controller, 0.081 m. A similar trend is witnessed for BA and DTL values. The complete results are presented elsewhere. The input voltages for the three controlled systems are compared in Fig. 8. The results show clearly that the proposed fuzzy logic controller has the lowest root mean square (RMS) of the input voltages.

Table 4: PTP values of SWS, BA and DTL under road bump excitation at 0.856 m/s

System type	SWS (m)	BA (m/s^2)	DTL (N)
Conv. passive	0.0916	6.4195	1609
MR passive	0.0635	6.1393	1537
SAS On-Off	0.0620	5.9943	1491
SAS Skyhook	0.0481	4.7651	1275
SAS Fuzzy logic	0.0329	3.5464	-

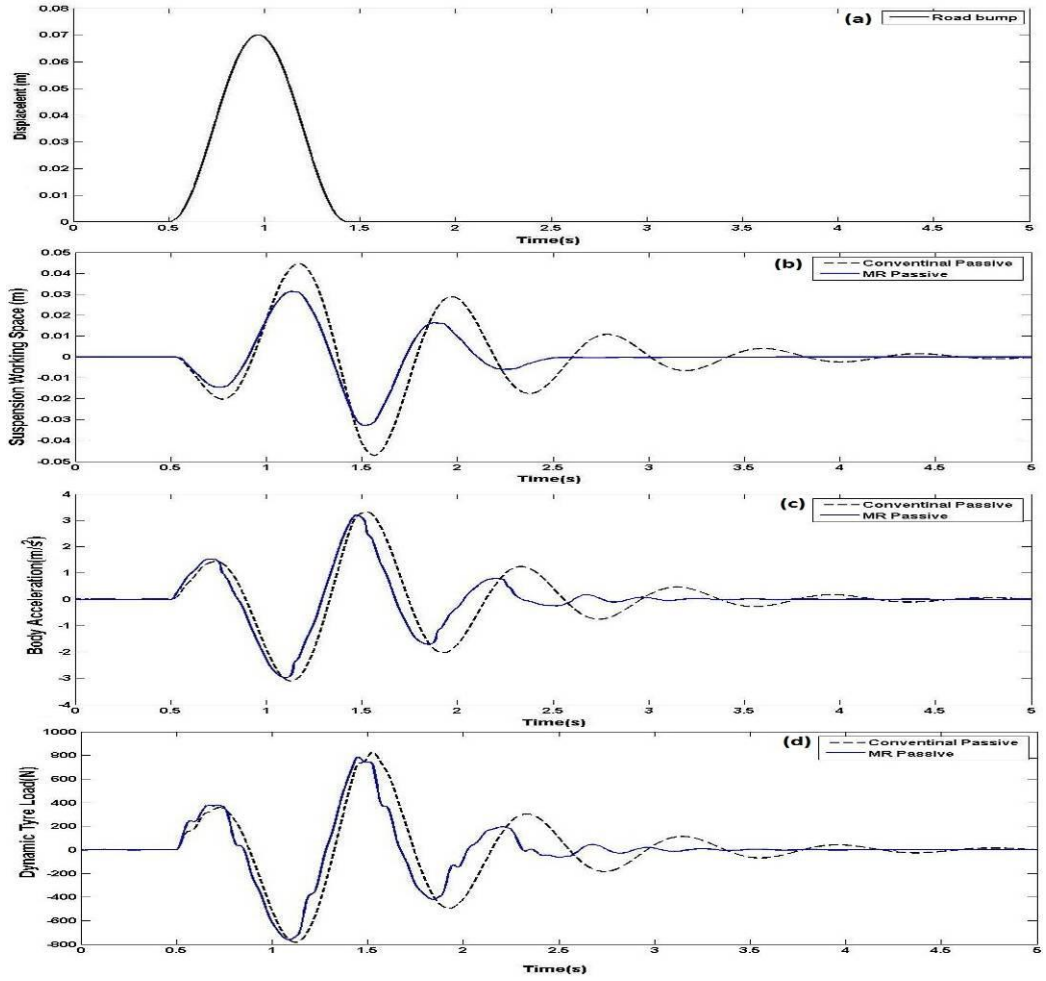

Fig. 6: Suspension system responses with conventional and MR passive dampers - (a) Road excitation; (b) SWS; (c) BA; (d) DTL

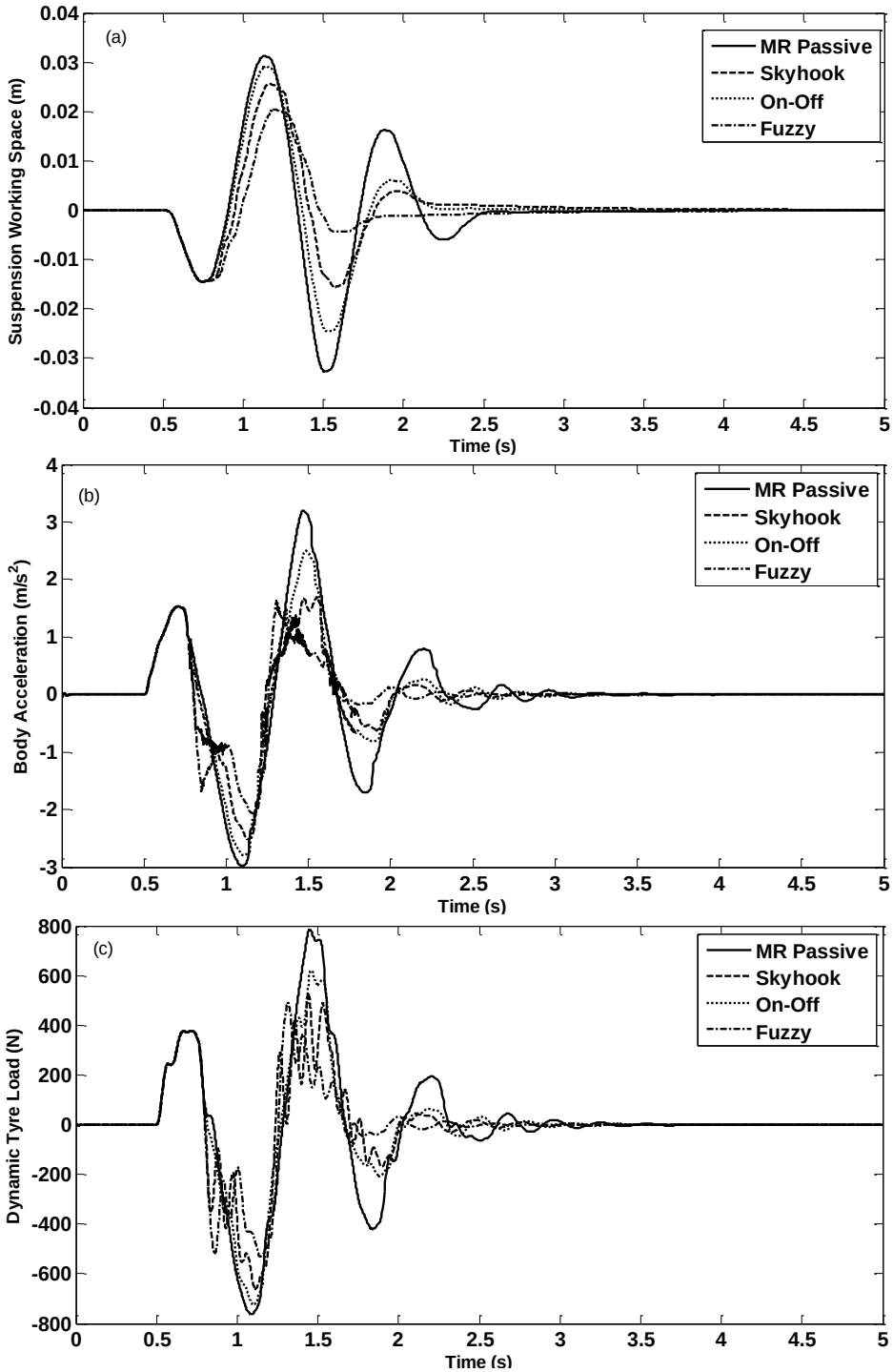

Fig. 7: Time histories of SAS system response for various control techniques under road bump excitation - (a) SWS; (b) BA; (c) DTL

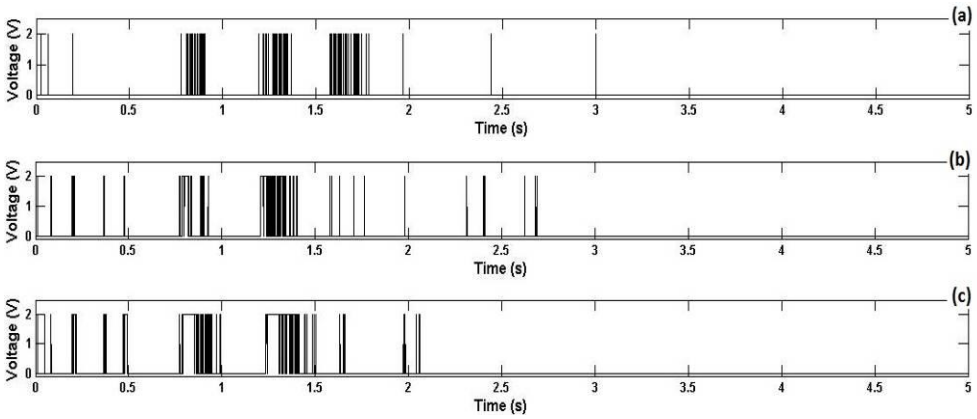

Fig. 8: Voltage applied to MR damper by different controllers - (a) On-Off; (b) Skyhook; (c) Fuzzy logic

The second type of road excitation is a random road profile described as:

$$\dot{y}_r + \rho V y_r = V W_n \quad (16)$$

Where W_n is a white noise with an intensity of $2\sigma^2\rho V$. ρ is the road irregularity factor. σ^2 is the covariance of road irregularity. Assuming that the vehicle maintains a constant velocity of *V=20 m/s* on the road, the values [29] of the road surface irregularity were selected as: ρ = 0.45 m^{-1} and σ^2=300 mm^2. In order to improve the ride comfort, it is important to isolate the vehicle body from the road disturbances and to decrease the resonance peak of the body mass near 1Hz, which is known to be a sensitive frequency to the human body [2, 30]. Moreover, in order to improve the vehicle stability, it is important to keep the tyre in contact with the road surface and therefore to decrease the resonance peak near 10Hz, which is the resonance frequency of the wheel [2, 30]. In view of these considerations, the results obtained for the excitation described by Eqn. (16) are presented in the frequency domain. The modulus of the Fast Fourier Transforms (FFT) of the SWS, BA, and DTL responses in the range of 0.5-15 Hz are used to compare different controllers. The FFT was scaled and smoothed by curve-fitting as done by Metered et al. [20].

The FFT plots in Figs. 9 and 10 show that the lowest resonance peak is achieved by the proposed fuzzy logic controller. The suspension system with fuzzy logic controller can properly dissipate the energy due to random road excitation. RMS values of the SWS, BA and DTL are presented in Table 5 and shows that the SAS systems have led to lower RMS values compared with conventional passive damper. This demonstrates their ability to enhance the ride comfort and vehicle stability. The results also suggest a satisfactory performance from the system with passive MR damper. The input voltages for the three controlled systems are compared in Fig. 11 under random road excitation. The results clearly show that the proposed fuzzy logic controller has the lowest RMS of input voltages.

Table 5: RMS values of SWS, BA and DTL responses under random road excitation

System Type	SWS (m)	BA (m/s^2)	DTL (N)
Conv. Passive	0.0081	1.35	432.41
MR Passive	0.0059	1.115	413.49
SAS On-Off	0.0063	1.14	402.47
SAS Skyhook	0.0051	0.984	346.39
SAS Fuzzy logic	0.0047	0.803	311.49

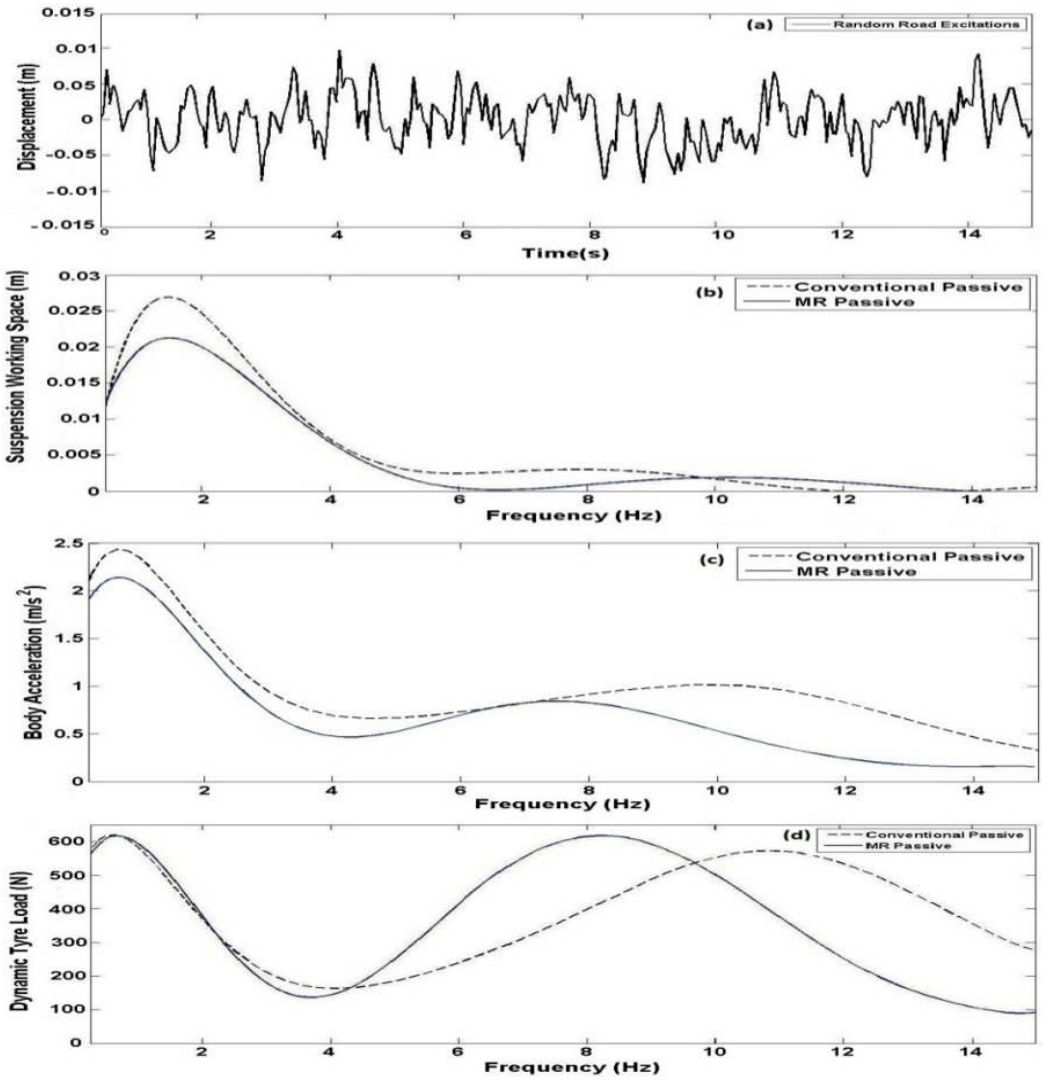

Fig. 9: Modulus of Fast Fourier Transform of performance criteria for passive system response under random road excitations - (a) Random road excitation profile; (b) SWS; (c) BA; (d) DTL

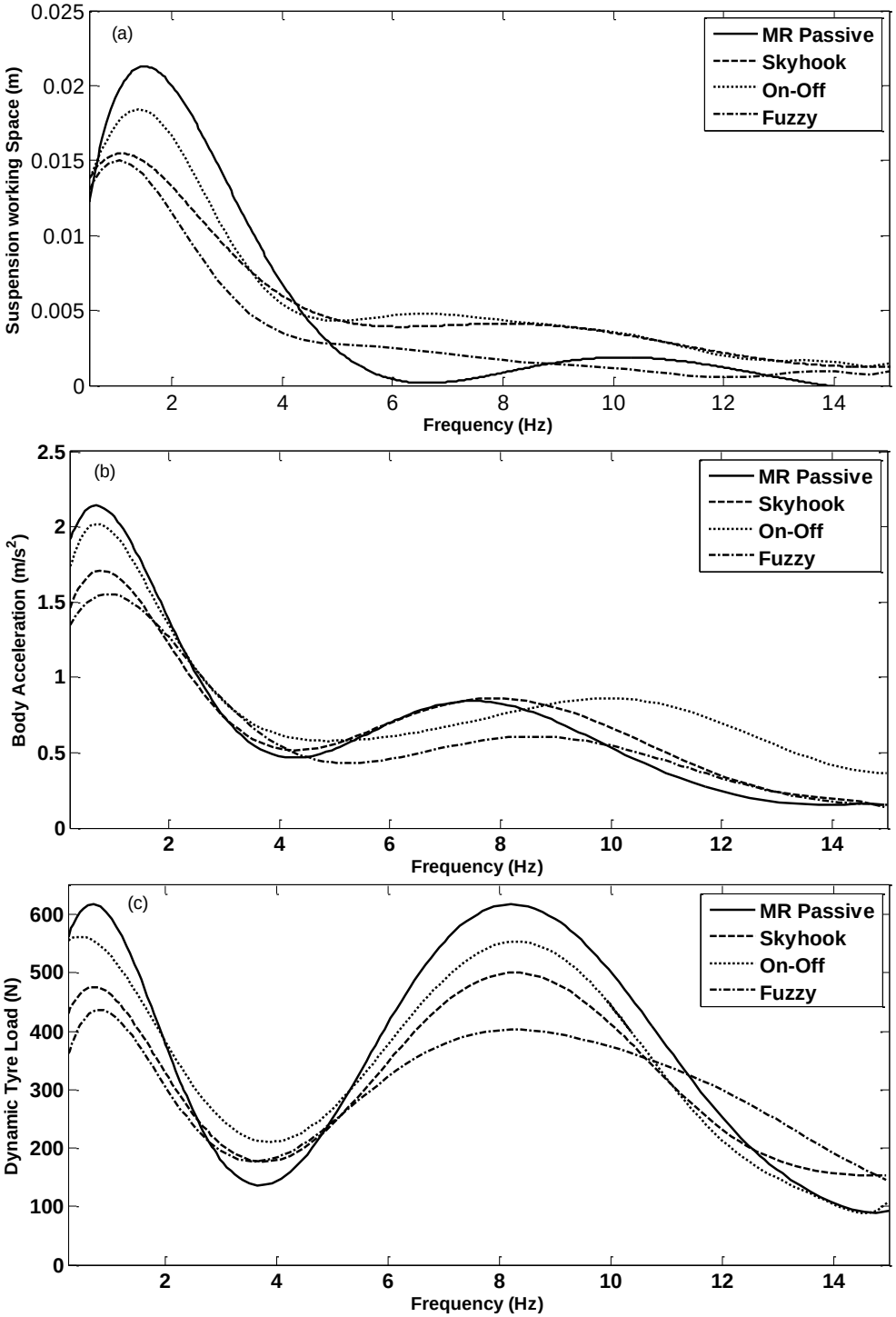

Fig. 10: Modulus of the Fast Fourier Transform (FFT) of performance criteria for SAS system response under random road excitations for various controllers. (a) SWS; (b) BA; (c) DTL

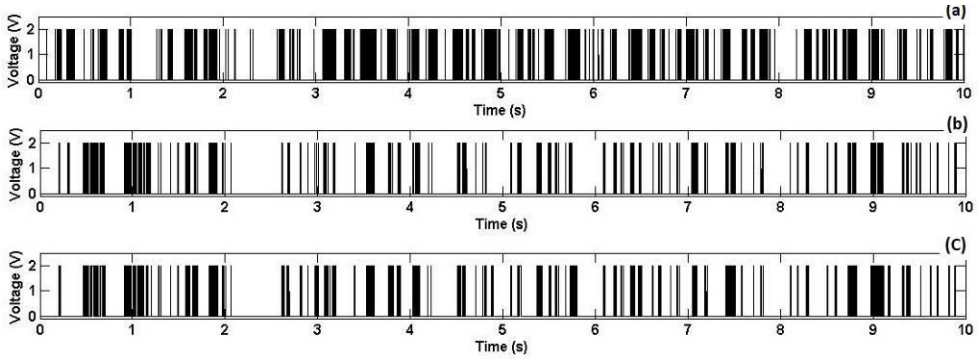

Fig. 11: Voltage applied to MR damper by different controllers (a) On-Off; (b) Skyhook; (c) Fuzzy logic

6. Experimental results and discussion

A test rig based on a 2 DoF quarter car suspension was designed for the purpose of the experimental investigation. Figs. 12(a) to (c) show the configuration of the quarter car elements of the rig. The stiffness in the suspension and tyre are created by two parallel springs rather than one spring. The damper is moved to the middle point in between the sprung and unsprung masses to achieve better stability of the test rig structure. Linear bearing blocks are used as the sprung and unsprung masses that can vertically slide on the guide shafts. The test rig is designed based on the parameters given in Table 6. It should be noted that due to the significant difference between the operating range of conventional shock absorbers in the market and those available in our laboratory and due to design restrictions, the test rig accommodates the MR damper only. This in turn imposes the use of a passive MR damper as the basis for the comparison of different control strategies.

Table 6: Test rig parameters

Parameter	Symbol	Value
Sprung Mass	M_s	24 kg
Unsprung Mass	M_u	5.4 kg
Suspension stiffness	$K'_s=2K_s$	2.4 kN/m
Tyre stiffness	$K'_t=2K_t$	24 kN/m

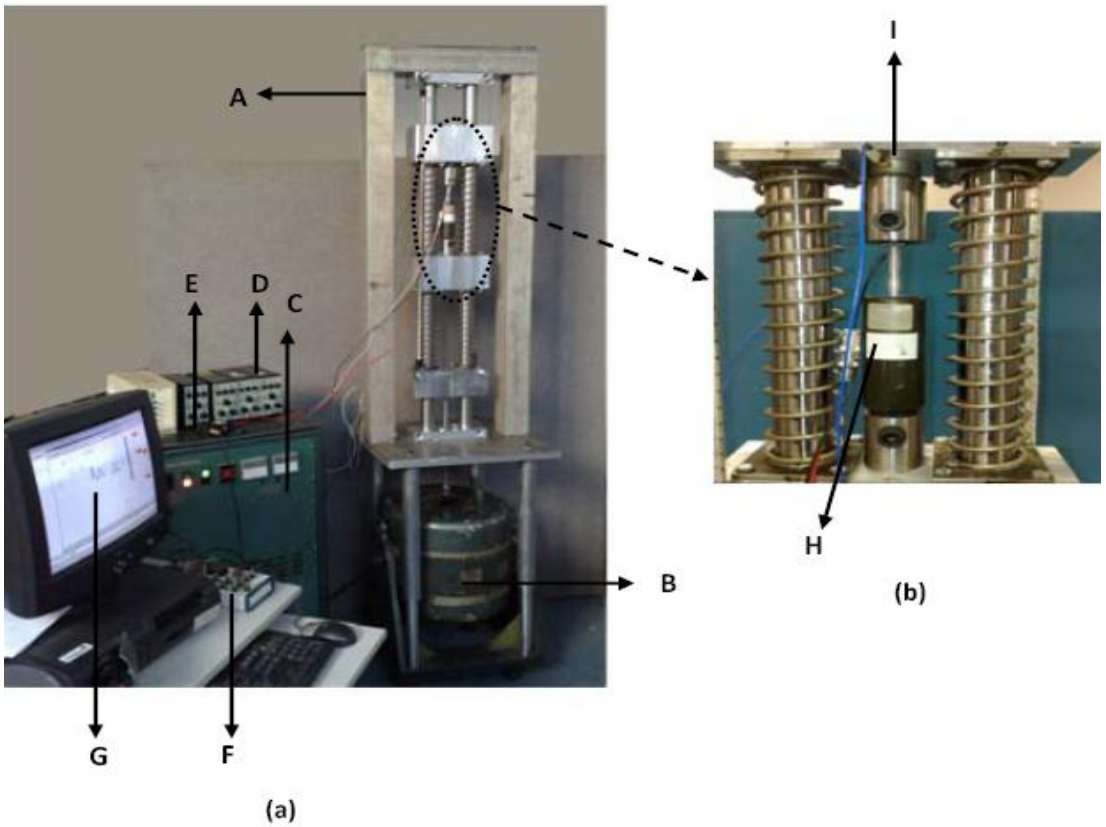

Fig. 12: Experimental setup - (a) Test rig photo (b) test rig zoomed view. A: Quarter car test rig, B: Electromagnetic shaker, C: Power amplifier, D: Charge amplifiers, E: MR damper driver, F: NI connection card, G: Computer with MATLAB Real Time Workshop, H: MR damper mounted on the test rig, I: Force gauge washer.

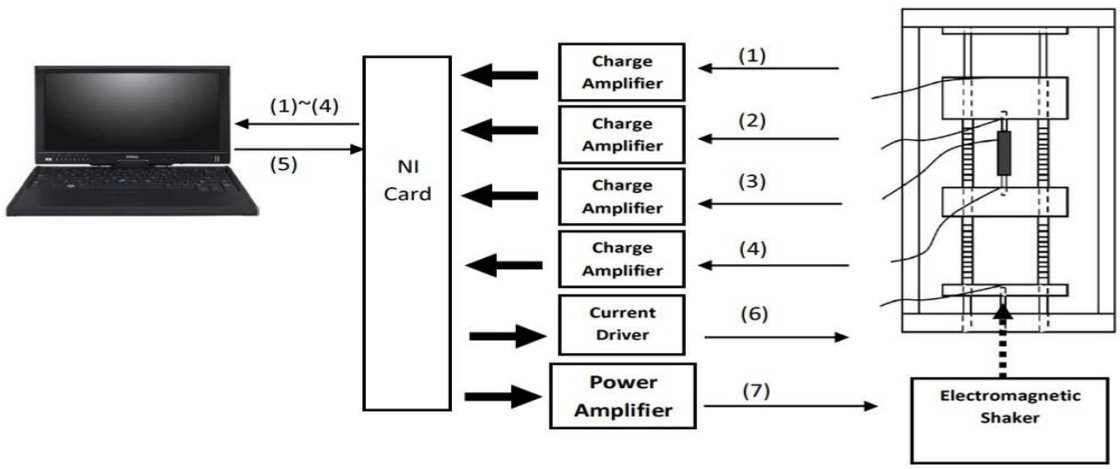

Fig. 12(c): Experimental setup - Arrangement of elements in experimental setup. (1): Sprung mass acceleration signal, (2): Unsprung mass acceleration signal, (3): Excitation plate acceleration signal, (4): MR damper force signal, (5): Computer programme output composed of (6): MR damper voltage command signal and (7): Excitation signal.

Three accelerometers are placed on the mass blocks and the excitation plate to measure the acceleration shown by signal (1) to (3) in Fig. 12(c). The acceleration signals along with the MR damper force signal (4) from the force gauge are then amplified in charge amplifiers and sent to the NI connection card which is used as the system interface. The charge amplifiers are equipped with analogue integration capability and can convert the acceleration signals to speed or displacement as required. The processed signals (5) are then sent to the computer where the magnitude of the voltage to the MR damper is varied according to the controller techniques. The output signal (5) is composed of the voltage command (6) to the current driver of the MR damper and signal (7) that refers to the excitation signal. The excitation signal is amplified by the shaker's power amplifier too and excites the electromagnetic shaker. The road displacement was simulated by a Gaussian white-noise signal of 0-3Hz band [31] with ± 0.02m amplitude [6].

Time histories of the test rig response in terms of SWS and BA performance criteria are recorded and plotted in Fig. 13. Current design of the test rig allows measurement of SWS and BA only. Measuring DTL required adding extra features to the test rig and will be addressed in the future. A controlled damper has noticeably improved the system response regardless of the control strategy. The proposed fuzzy logic controller has significantly limited the sprung mass accelerations and inhibited its variations. The RMS values of the system responses are summarized in Table 7. The fuzzy logic controller is the most efficient controller in restricting the accelerations. The pattern of applied voltage to MR damper by different controllers is plotted in Fig. 14 for comparison. Due to the nature of the excitation, the voltage signals repeatedly changes between 0 to 2V throughout the excitation period. Different controllers apply the voltage at different intervals with different durations and results in different system behaviour.

Table 7: RMS of SWS and sprung mass acceleration

System Type	SWS (m)	Sprung mass Acceleration (m/s^2)
MR Passive	0.0113	1.5670
SAS On-Off	0.0106	1.1253
SAS Skyhook	0.0089	0.8242
SAS Fuzzy logic	0.0071	0.6043

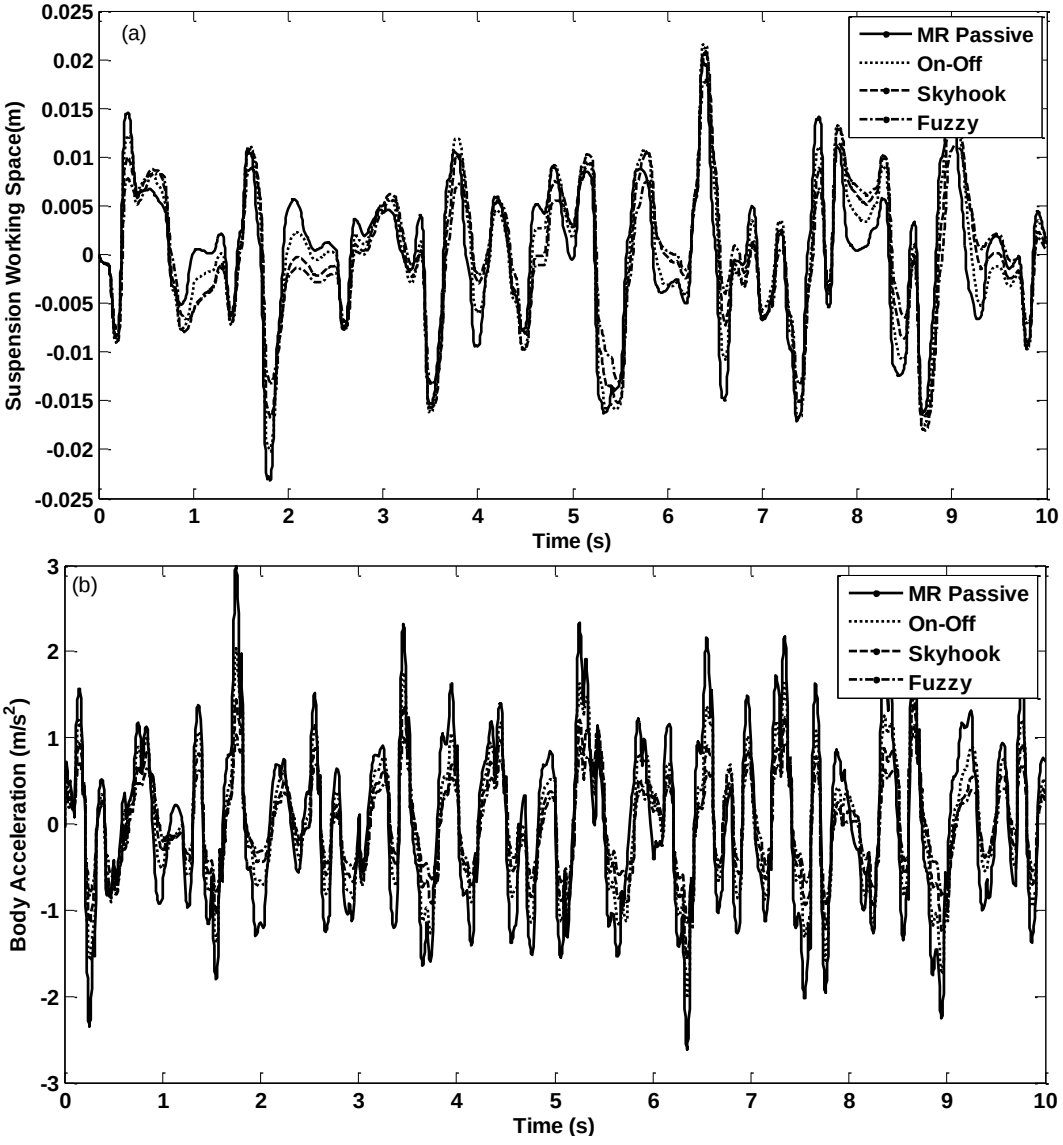

Fig. 13: Time histories of SAS system response under random road excitations - (a) SWS; (b) BA

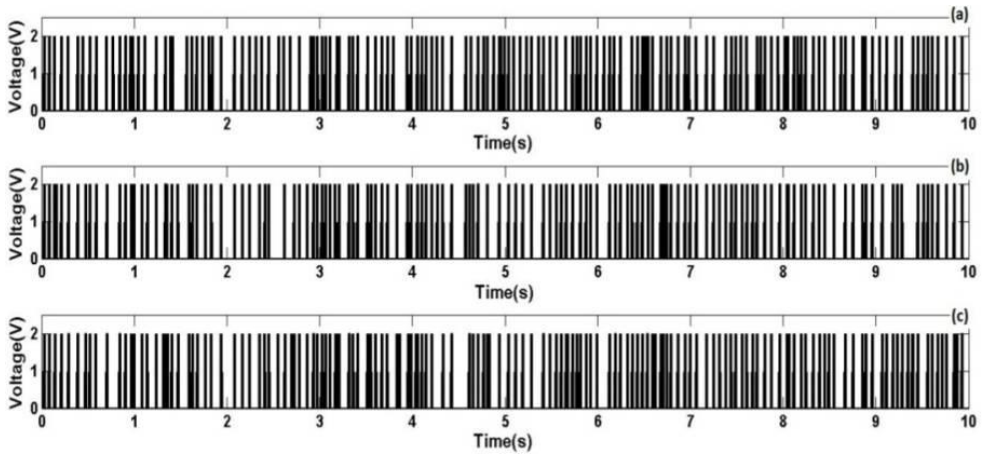

Fig. 14: Voltage applied to MR damper by different controllers through experiments - (a) On-Off; (b) Skyhook; (c) Fuzzy logic

7. Conclusions

This paper introduced theoretical and experimental investigation of a controlled SAS quarter car model incorporating MR Damper. A 2 DoF model of a semi-active quarter vehicle suspension system using an MR damper was derived. The control technique is composed of a system controller and a damper controller. Different system controller types including a fuzzy logic controller were employed in conjunction with a Heaviside step function damper controller. The suspension system performance criteria were assessed using different system controller types based on the dynamic response of a quarter car model/suspension in the time and frequency domains in order to quantify the suspension effectiveness under bump and random road disturbance. Studies using the Modified Bouc-Wen model for the MR damper, as well as an actual damper fitted in a complete quarter car suspension test rig, both showed that the proposed fuzzy logic system controller potentially offers significantly superior ride comfort and vehicle stability over the other system controllers applied in this investigation.

REFERENCES:

[1] A. Alleyne, P.D. Neuhaus and J.K. Hedrick. 1993. Application of nonlinear control theory to electronically controlled suspensions, *Vehicle Sys. Dynamics*, 22(5-6), 309-320. http://dx.doi.org/10.1080/00423119308969033.

[2] T.D. Gillespie. 1993. *Fundamentals of Vehicle Dynamics*, SAE Int.

[3] D. Karnopp, M.J. Crosby and R.A. Harwood. 1973. Vibration control using semi-active force generators, *ASME J. Manuf. Sci. Eng*, 96(2), 619-626.

[4] K. Yi and B.S. Song. 1999. New adaptive sky-hook control of vehicle semi-active suspension, *J. Automobile Engineering*, 213(3), 293-303. http://dx.doi.org/10.1243/0954407991526874.

[5] B.F. Spencer Jr., S.J. Dyke, M.K. Sain and J.D. Carlson. 1996. Phenomenological model of magneto-rheological damper, *J. Engineering Mechanics*, 123(3), 230-238.

[6] H. Metered, P. Bonello and S.O. Oyadiji. 2009. The experimental identification of magneto-rheological dampers and evaluation of their controllers, *Mechanical Systems and Signal Processing*, 24, 976-994. http://dx.doi.org/10.1016/j.ymssp.2009.09.005.

[7] W.W. Chooi and S.O. Oyadiji. 2008. Design, modelling and testing of magneto-rheological (MR) dampers using analytical flow solutions, *Computers & Structures*, 86(3-5), 473-482. http://dx.doi.org/10.1016/j.compstruc.2007.02.002.

[8] D. Simon and M. Ahmadian. 2001. Vehicle evaluation of the performance of magneto-rheological dampers for heavy truck suspensions, *J. Vibration and Acoustics*, 123(3), 365-375. http://dx.doi.org/10.1115/1.137672.

[9] N. Al-Holou and A. Bajwa. 1994. Computer controlled individual semi-active suspension system, *IEEE Proc. 36th Midwest Symp. Circuits and Systems*, Detroit, USA.

[10] S.M. Savaresi, E. Silani, S. Bittanti and N. Porciani. 2003. On performance evaluation methods and control strategies for semi-active suspension systems, *Proc. 42nd IEEE Conf. Decision and Control*, Maui, Hawaii, USA.

[11] H.S. Lee and B.S. Choi. 2000. Control and response characteristics of a magneto-rheological fluid damper for passenger vehicles, *Intelligent Materials Systems and Structures*, 11, 80-87. http://dx.doi.org/10.1177/1045389900772664422.

[12] M. Ahmadian and C.A. Pare. 2000. A quarter-car experimental analysis of alternative semi-active control methods, *Intelligent Materials Systems and Structures*, 11, 604-612. http://dx.doi.org/10.1106/MR3W-5D8W-0LPL-WGUQ.

[13] Y. Shen, M.F. Golnaraghi and G.R. Heppler. 2006. Semi-active vibration control schemes for suspension systems using magneto-rheological dampers, *J. Vibration and Control*, 12(1), 324. http://dx.doi.org/10.1177/1077546306059853.

[14] D. Sammier, O. Sename and L. Dugard. 2003. Skyhook and H∞ control of semi-active suspensions: some practical aspects, *Vehicle System Dynamics*, 39(4), 279-308. http://dx.doi.org/10.1076/vesd.39.4.279.14149.

[15] X. Song, M. Ahmadian, S. Southward and L.R. Miller. 2005. An adaptive semiactive control algorithm for magneto-rheological suspension systems, *J. Vibration and Acoustics*, 127(5), 493-502. http://dx.doi.org/10.1115/1.2013295.

[16] D.L. Guo, H.Y. Hu and J.Q. Yi. 2004. Neural network control for a semi-active vehicle suspension with a magneto-rheological damper, *J. Vibration and Control*, 10(3), 461-471. http://dx.doi.org/10.1177/1077546304038968.

[17] W.H. Liao and D.H. Wang. 2003. Semiactive vibration control of train suspension systems via magneto-rheological dampers, *J. Intelligent Material Systems and*

Structures, 14(3), 161-172. http://dx.doi.org /10.1177/1045389X03014003004.

[18] H. Metered. 2012. Application of nonparametric magneto-rheological damper model in vehicle semi-active suspension system, *SAE Int. J. Passenger Cars - Mech. Syst.*, 5(1), 715-726.

[19] A.H. Lam and H.W. Liao. 2003. Semi-active control of automotive suspension systems with magneto-rheological dampers, *Int. J. Vehicle Design*, 33, 50-75. http://dx.doi. org/10.1504/IJVD.2003.003652.

[20] H. Metered, P. Bonello and S.O. Oyadiji. 2010. An investigation into the use of neural networks for the semi-active control of a magneto-rheologically damped vehicle suspension, *J. Automobile Engineering*, 224(7), 829-848. http://dx.doi.org/10.1243/09544070JAUTO1481.

[21] N. Al-Holou and A. Shaout. 1994. The development of fuzzy logic based controller for semi-active suspension system, *Proc. 37th Midwest Symp. Circuits and Systems*, Lafayette, USA.

[22] C. Nicolas, J. Landaluze, E. Castrillo, M. Gaston and R. Reyero. 1997. Application of fuzzy logic control to the design of semi-active suspension systems, *Proc. IEEE Int. Conf. Fuzzy Systems*, 2, 987-993.

[23] S.Y. Bei. 2009. Fuzzy controller for automotive semi-active suspension based on damping control, *Proc.* 2nd *Int. Colloquium Computing, Communication, Control, and Management*, Sanya, China.

[24] M. Yu, C.R. Liao, W.M. Chen and S.L. Huang. 2006. Study on MR semi-active suspension system and its road testing, *J. Intelligent Material Systems and Structures*, 17, 801-806. http://dx.doi.org/10.1177/1045389X060 57534.

[25] S.J. Dyke, B.F. Spencer Jr, M.K. Sain and J.D. Carlson. 1996. Modelling and control of magneto-rheological dampers for seismic response reduction, *Smart Materials and Structures*, 5, 565-575. http://dx.doi.org/10.1088/09 64-1726/5/5/006.

[26] M.M. Biglarbegian and F.A. Golnaraghi. 2008. Novel neuro-fuzzy controller to enhance the performance of vehicle semi-active suspension systems, *J. Vehicle System Dynamics*, 46(8), 691-711. http://dx.doi.org/10. 1080/00423110701585420.

[27] S. Turkay and H. Akuay. 2005. A study of random vibration characteristics of the quarter-car model, *J. Sound and Vibration*, 282(1-2), 111-124. http://dx.doi. org/10.1016/j.jsv.2004.02.049.

[28] D.C. Karnopp and M.J. Crosby. 1974. *System for Controlling the Transmission of Energy between Spaced Members*, US Patent Number 3807678.

[29] S.B. Choi and W.K. Kim. 2000. Vibration control of a semi-active suspension featuring electro-rheological fluid dampers, *J. Sound and Vibration*, 234, 537-546. http://dx.doi.org/10.1006/jsvi.1999.2849.

[30] D. Fischer and R. Isermann. 2004. Mechatronic semi-active and active vehicle suspensions, *Control Engineering Practice*, 12(11), 1353-1367. http://dx.doi. org/10.1016/j.conengprac.2003.08.003.

[31] S.B. Choi, H.S. Lee and Y.P. Park. 2002. H-infinity control performance of a full-vehicle suspension featuring magneto-rheological dampers, *Vehicle System Dynamics*, 38(5), 341-360. http://dx.doi.org/10.1076/ vesd.38.5.341.8283.